Published in final edited form as:

JACC Cardiovasc Imaging. 2019 April ; 12(4): 665–677. doi:10.1016/j.jcmg.2017.09.013.

Mitral Valve Adaptation to Isolated Annular Dilation: Insights into the Mechanism of Atrial Functional Mitral Regurgitation

Dae-Hee Kim, MD, PhD[a,*], **Ran Heo, MD**[a,*], **Mark D. Handschumacher, BS**[b], **Sahmin Lee, MD, PhD**[a], **Yun-Sil Choi, RN, RDCS**[a], **Kyu-Ri Kim, RN, RDCS**[a], **Yewon Shin, RN, RDCS**[a], **Hong-Kyung Park, RN, RDCS**[a], **Joyce Bischoff, Ph.D**[c], **Elena Aikawa, M.D., PhD**[d], **Jong-Min Song, MD, PhD**[a], **Duk-Hyun Kang, MD, PhD**[a], **Robert A. Levine, MD**[b,†], and **Jae-Kwan Song, MD, PhD**[a,†]

[a]Cardiac Imaging Center, Asan Medical Center Heart Institute, University of Ulsan College of Medicine, Seoul, South Korea

[b]Cardiac Ultrasound Laboratory, Massachusetts General Hospital, Harvard Medical School, Boston, Massachusetts, USA

[c]Vascular Biology Program and Department of Surgery, Boston Children's Hospital, Harvard Medical School, Boston, MA, USA

[d]Center for Excellence in Vascular Biology, Division of Cardiovascular Medicine, Brigham and Women's Hospital, Harvard Medical School, Boston, MA, USA

Abstract

Objectives—We hypothesized that compensatory MLA adaptation occurs in patients with persistent AF without LV dysfunction but has limitations that augment MR. We also explored whether asymmetric annular dilation is matched by relative leaflet enlargement.

Background—Functional mitral regurgitation (MR) occurs in patients with atrial fibrillation (AF) and isolated annular dilation, but the relation of mitral leaflet surface area (MLA) adaptation to annular area is unknown.

Methods—3D echocardiographic images were acquired from 86 patients with quantified MR: 53 with non-valvular persistent AF (23 MR+ with ≥ moderate MR, 30 MR−) without LV dysfunction or dilation and 33 normal controls. Comprehensive 3D analysis included total diastolic MLA,

Corresponding author: Dae-Hee Kim, MD, PhD, Associate Professor of Medicine, Asan Medical Center Heart Institute, University of Ulsan College of Medicine, 388-1 Poongnap-dong Songpa-gu, Seoul, 138-736, South Korea, Phone: 82-2-3010-3151, Fax: 82-2-486-5918, daehee74@amc.seoul.kr.

*These first authors contributed equally

†Senior authorship is acknowledged for Drs RA Levine and JK Song to reflect this cross-disciplinary collaboration and their unique contributions

Disclosures: none

This study was supported by research grant from the Korean Society of Echocardiography, in part by NIH grants R01 HL128099 and HL141917, and by support from the Ellison Foundation, Boston, MA.

adaptation ratios: MLA to annular area and MLA to leaflet closure area, and annular and tenting geometry.

Results—Total MLA was 22% larger in AF patients than controls, paralleling increased annular area (AA). However, as AA increased, adaptive indices (MLA/AA and MLA/closure area) plateaued, becoming lowest in MR+ patients (MLA/closure area =1.63±0.17 controls, 1.60±0.11 MR−, 1.32±0.10 MR+, $p<0.001$). MR increased as MLA/closure area decreased ($R^2=0.68$, $p<0.001$). The posterior:anterior MLA ratio remained constant while posterior:anterior MA perimeter increased (1.21±0.16 controls, 1.32±0.20 MR−, 1.46±0.19 MR+, $p<0.001$). Multivariate MR determinants were annular area, total MLA to closure area and posterior:anterior perimeter ratios.

Conclusions—MLA adaptively increases in AF with isolated annular dilation and normal LV function. This compensatory enlargement becomes insufficient with greater annular dilation, and the leaflets fail to match asymmetric annular remodeling, increasing MR. These findings can potentially help optimize therapeutic options and motivate basic studies of adaptive growth processes.

Keywords

mitral valve; atrial fibrillation; mitral regurgitation; mitral annulus; three-dimensional echocardiography

---

The ability of heart valves to adapt to expansion of their surrounding structures is increasingly recognized. MV surface area increases as the LV dilates in aortic insufficiency (AI), preventing MR (1,2). In LV dysfunction with remodeling, papillary muscle (PM) displacement tethers the leaflets and restricts their closure, producing functional MR (FMR) (3,4); MV surface area also exceeds normal, but varies among patients, and those with smaller leaflet areas have more MR(1,5). Leaflet tethering by mechanically displaced PMs without myocardial infarction (MI) causes adaptive MV growth (6,7); but in the infarcted ventricle, compensatory valve growth appears limited by pro-fibrotic processes (6). AV surface area similarly increases with aortic root dilation but plateaus at larger aortic areas and fails to match asymmetric sinus enlargement, causing relative leaflet deficiency and AI (8).

Atrial fibrillation (AF) causes annular dilation without LV dysfunction or dilation(9). It has been controversial whether isolated annular dilation in AF is sufficient to cause significant (moderate or greater) FMR (10–12). However, there are patients with significant "atrial FMR" caused by AF with annular dilation and without LV dysfunction (13–17)(Figure 1). Annular dilation has also been recognized by surgeons as the cause of Carpentier type I MR (18), but its mechanism requires further study of three-dimensional leaflet and annular geometry(15). Understanding the mechanism of atrial FMR is important due to its consequences as a surgical indication and potential stimulus for recurrent AF despite ablation (11,19,20).

To address the central question of mitral leaflet adaptation requires measuring total mitral leaflet area (MLA), which can be determined precisely only in diastole because in systole, the area of each leaflet involved in coaptation cannot be optimally resolved. Measuring

diastolic MLA also evaluates adaptation when LV pressure and leaflet tension are minimal without the passive stretch that occurs during systole (21,22). Leaflet adaptation can then be determined by comparing total MLA with the tented area needed to close the annular orifice in systole as determined by the net leaflet tethering created by the PMs and dilating annulus (5,23). The strongest predictor of FMR in LV dysfunction is a reduced ratio of total diastolic MLA to mid-systolic closure area (5,23).

One recent paper has measured closed leaflet areas at early and late systole and showed larger areas in AF patients with significant MR versus normal controls (16). However, both systolic areas are influenced by systolic stretch. Another recent paper focused on end-systolic closed leaflet area, which depends strongly on the degree of tethering for any given total area (17). To date, we lack information on how MLA increases in response to increasing annular area. This motivated us to explore open and closed leaflet areas in patients with AF both with and without MR and therefore with a range of annular areas. This study used 3D echocardiography to address the hypothesis that MLA *increases in AF as the annulus dilates, but this adaptation may plateau at larger annular areas, with the resulting leaflet deficiency causing functional MR*. As part of this hypothesis, we explored whether *asymmetric* and typically posterior-predominant *annular dilation* is matched by posterior relative to anterior leaflet enlargement.

Methods (See supplemental material)

Study population

Among 1247 consecutive patients with persistent non-valvular AF referred for echocardiography between November 2010 and February 2012, we identified 53 patients with ≥moderate MR, normal EF (≥50%), normal EDV index (≤75 ml/cm^2) and no regional wall motion abnormalities. Exclusions, such as organic MV disease, patients with current or previous history of heart failure, LV dysfunction or dilation, left an MR+ group of 23 patients with ≥moderate MR, who were compared with 30 patients of similar age with non-valvular AF and no significant MR or LV dysfunction (MR- group) and 33 normal subjects. All patients gave written informed consent. We also analyzed seven sets of follow-up 3D images available in the same patients with a median follow-up of 4.8 years.

Echocardiography

Transthoracic echocardiography was obtained with an iE33 scanner. LV volumes were assessed by the biplane Simpson's method. MR was assessed using an integrative approach, with the primary measurement of vena contracta width (VCW), correlated with the proximal flow convergence method (24). Single-beat full volume datasets (median 10, IQR [9–11] fps) were acquired in AF patients and three consecutive beats were averaged. ECG-gated full volume images were acquired over four consecutive cardiac cycles in normal subjects (median 24, IQR [22–26] fps). Maximal 3D LA volume was measured offline (25). Anterior and posterior leaflet thicknesses were measured in the 4-chamber view in the mid-leaflet at end diastole (5).

MLA (Figure 2)

Total MLA was assessed at full diastolic-opening, and closure area, which represents the minimal area that needs to be covered by the leaflets to occlude the mitral orifice, was measured at mid-systole (1,5,6,23,26,27). 3D analyses were performed with customized software (Omni 4D, MDH), the operators blinded to MR severity. To test whether leaflet area increased relative to changes in annular area, we calculated the ratio of leaflet to AA in diastole. To assess the adequacy of leaflet adaptation to that needed for closure, we calculated the ratio of total open to leaflet closure area (1,5).

Mitral annular geometry and function (Figure 3)

Mitral annular cross-sectional area (AA) was measured at mid-systole & mid-diastole, and its fractional area change was calculated as: (mid-diastole – mid-systole)/mid- systole) *100. Annular height (27), inter-commissural (IC) and antero-posterior (AP) diameters were measured, circularity index calculated as AP/IC. 3D annular perimeter (28)and its anterior and posterior circumferences were calculated. Four annular quadrants were measured based on the medial and lateral commissural points and the intersections of the annulus with an antero-posterior line connecting the AV-MV centroids. Quadrants were summated to obtain posterior and anterior perimeters (Q2+Q3 and Q1+Q4). Q2/Q3 ratio expressed medial-to-lateral posterior annular asymmetry.

Tenting geometry

Tenting volume was determined by tracing MV leaflet surfaces at mid-systole. As shown in Figure 6A, the position of the maximally tented (most apical) point of the leaflets was measured along the axes of the annular plane, with the Y-axis connecting the MV-AV centroids. The anterior and posterior leaflet tenting angles were measured as described (29).

Reproducibility

All geometric parameters including MLA were consistently measured by one physician (D.-H.K.), and variability was compared with blinded measurements of another observer (Y.-S.C.). Intra- and inter-observer variability were assessed between the two independent observers for 15 randomly selected subjects (5 from each group). For test-retest reproducibility (validation), we analyzed 15 patients with persistent AF who had both transthoracic and transesophageal 3D echocardiographic studies, comparing total MLA, closure area and AA between both tests.

Statistical analysis (Supplemental material)

Statistical significance among the three groups was determined using one-way ANOVA or Kruskal-Wallis test and post-hoc analysis with Bonferroni correction. A binary logistic regression analysis and an internal validation with bootstrap (1000 replicates) were performed to find the determinants of significant MR. For test-retest reproducibility, we performed linear regression and Bland–Altman analysis to compare 3D TTE and TEE measurements. Intraclass correlation coefficient and coefficient of variation were calculated for the inter-, intra-observer variability and agreement between the two tests (SAS 9.1, Cary, NC).

Results

Baseline characteristics & echocardiographic measures (Table 1)

The three groups were similar with respect to age and body surface area. Blood pressure was slightly lower in AF groups, while heart rate was slightly faster in MR+ group. Medication use was not different between MR+ and MR- groups. In MR+ group, 83% of patients had moderate MR; VCW was 5.1±1.2mm. There was no significant difference in LVEDV index among three groups; whereas EF was slightly lower in AF groups. LA volume index was larger in patients with AF compared with normal, and larger in MR+ than MR- group. Leaflet thickness was greater in AF groups, but not different between MR+ and MR- groups.

MLA (Table 2)

Total open MLA was significantly (22%) larger in patients with AF compared with normal, and larger in MR+ versus MR- group (15.5±2.1, 14.3±1.9 vs. 12.1±1.5 cm^2, $p<0.001$). (Please see examples in Figure 2.) The anterior to posterior MLA ratio was not different among three groups.

Adequacy of leaflet adaptation

Total MLA increased in parallel with AA increase, but declined mildly below the regression line at higher AAs (Figure 4, upper left). Leaflet closure area likewise increased with AA, but rose mildly above the regression line at higher AAs (upper right). Total MLA to AA ratio in MR- group was similar with that of normals (Table 2), suggesting adequate leaflet adaptation to lesser degrees of annular dilation. In contrast, total MLA to AA ratio decreased in MR+ group from the normal range of 1.5–2.0 to <1.5, with a lower plateau in this ratio at higher AAs (lower left).

Similarly, total to closure leaflet area ratio was comparable in MR- and normal groups but lower in MR+ group (1.63±0.17, 1.60±0.11 vs. 1.32±0.10, $p<0.001$). The total to closure ratio showed a continuous decline as AA increased (Figure 4, lower right), also suggesting that adaptation becomes limited as the annulus dilates more prominently. Closure area increased to a greater extent than total leaflet area in the MR+ group (Figure 5A); total to closure area ratio correlated with VCW, which increased below a leaflet area ratio of 1.5 ($R^2=0.68$, $p<0.001$; Figure 5B).

Annular geometry

Systolic & diastolic AA were larger in patients with AF compared with normal, and larger in MR+ than MR- patients (Table 2). The fractional AA change was smallest in MR+ group, and smaller in MR- group that in normal. Annular diameters likewise increased in AF, with a more circular annulus (index closer to 1), highest in MR+ group. Annular nonplanarity angle was significantly increased in AF, and greatest in MR+ group, indicating a flatter annulus.

The posterior annulus perimeter increased as AA increased, unlike the anterior perimeter, so posterior to anterior perimeter ratio indicating asymmetric annular remodeling increased from 1.21±0.16 in normal to 1.32±0.20 in MR- and 1.46±0.19 in MR+ patients ($p<0.001$).

In contrast, the anterior-posterior leaflet areas ratio was constant (Figure 2, 4th column). Q2/Q3 ratio indicated no asymmetry between medial and lateral annulus.

Tenting geometry

Patients in MR+ group showed mild apical leaflet tenting (Figure 1, bottom panel); the anterior leaflet, normally concave toward the LV (upper two panels), became flattened. This is reflected in the significant but mild increase in tethering volume in MR+ versus MR- groups [2.1±0.8 vs. 1.3±0.5, p<0.001] (Figure 2, 3rd column), with the blue area in the lowest panel indicating greatest apical tethering. This mild tethering is also reflected in the tethering angles, especially for the posterior leaflet (39±7 for MR+ vs. 28±7° for MR- patients, p<0.001; 25±5 vs. 21±5° for the anterior, p<0.001). Posterior tenting angle correlated with VCW (R^2=0.35, p<0.001). The medio-lateral position (X-coordinate) of the maximally tented (apical) point of the valve was not significantly different among groups, but its anterior-posterior position (Y-coordinate) was located more posteriorly in the AF and especially MR+ groups, consistent with the maximal tenting point being displaced posteriorly as the annulus dilates in that direction (Figure 6). This Y-coordinate correlated mildly but significantly with AA (R^2=0.21, p<0.001).

Univariate and multivariate analysis

Table 3 summarizes logistic regression analysis for variables associated with significant MR (including three groups) in patients with AF. This revealed that AA, total MLA to closure area ratio and posterior to anterior annular perimeter ratio were independently associated with significant MR. In multivariate analysis including MR+ and MR- groups, total MLA to closure area ratio (OR: 0.119, 95% CI [0.030–0.430])and posterior to anterior annular perimeter ratio (OR:3.673, 95%CI [1.014–13.299]) were selected as independent determinants. Same variables were also chosen as independent determinants in all 1,000 bootstrap samples

Drug effect in the MR+ group

The MR+ patients who were taking ACE inhibitors or ARBs had a mildly greater total MLA to closure area ratio (1.36±0.09 vs. 1.28±07, p=0.024) and lower VCW (4.56±0.56 vs. 5.58±1.43 mm, p=0.038) compared with those not on such therapy.

Follow-up 3D imaging in a subset of the patient's group

Serial change of 3D parameters (7 pairs) between two-time points were presented in Table 4 Total MLA expansion (MLA) was significantly greater in patients whose MR remained trace compared with those who progressed to moderate MR (3.0±0.7 vs. 0.9±0.5 cm^2, p=0.006). The total MLA to closure area ratio at follow-up was significantly higher in MR progression- group (1.55±0.04 vs. 1.24±0.04, p<0.001) (Supplemental Figure 2C).

Reproducibility (Supplemental material)

For all parameters derived from 3D tracing, including MLA, the two independent observers reached an interobserver variability of 0.901–0.987 (intra-class correlation coefficients) and an intraobserver variability of 0.909–0.985. All measurements were within 10% coefficient

of variation (range: 3.7–9.6%). VCW and PISA radius, as two measures roughly related to the square root of orifice area or flow rate, correlated strongly (R^2=0.84, p<0.001).

In the validation study between TTE and TEE, there were excellent correlation and agreement for total MLA, closure area and AA between both modalities (Supplemental Fig 1).

Discussion

The results of this study show that in patients with AF, the mitral leaflets increase their area in response to isolated annular dilation without LV dysfunction or remodeling. However, this area increase becomes limited at larger AAs with a substantial decrease in the total leaflet area to AA ratio. MLA increase has the potential to adapt to isolated annular dilation in patients with AF and prevent MR; inadequate area increase, failing to match annular remodeling in extent or asymmetry, can augment tethering and MR. Moreover, we showed follow-up data, although in a subset of patients, which further support the hypothesis that failure of leaflet surface geometry expansion in face of a dilating annulus, creating MR (Figure 7). The increase in closure area is associated with tethering of the valve, consistent with its being stretched between an increasingly larger annulus and the undisplaced PMs. As a result, as the annulus dilates, there is progressive deficiency in leaflet area relative to that needed for effective closure, causing significant MR. There is also a failure of the valve to match the posterior-predominant annular dilation and remodeling.

Changes in annular circularity occur that may also limit closure of a valve designed to cover a D-shaped orifice (28). Annular flattening increases out-of-plane stresses transmitted to the leaflets (30), may compound their tethering while providing a potential stimulus for stress-induced growth.

Important new features of these findings include confirmation that total unstressed diastolic leaflet area is actually increased in AF; recognition of the limitation of compensatory mechanisms as AA increases among individuals and groups; demonstration of a quantitative relationship between the relative deficiency in the leaflet to closure area ratio and MR, quantified by complementary methods; and demonstration of inadequacy of valve adaptation to the changing annular configuration.

Whether atrial FMR is associated with tethering has not been clear in the past. It has similarly been unclear why the leaflets do not appear tethered in Carpentier type I MR due to annular dilation without LV dysfunction. Two recent papers regarding atrial FMR (12,16) describe apparently normal leaflet closure patterns in patients with MR; only one recent paper (17) suggests posterior leaflet tethering. Our data indicate that mild tethering of leaflets develops as AA and MR increase. This can be understood because the leaflets and chordae must extend over the three-dimensional space between the PMs and annulus, so that annular dilation tethers the leaflets even if the PMs are undisplaced. The absence of marked tethering can be explained on the basis of valve adaptation: as leaflet area expands, it compensates for annular dilation, acting to normalize leaflet position and reduce MR.

Limitations

Although this study shows that MLAs are larger in AF patients and proposed suggestive data that MLA increases over time in the same patients, a large number of further prospective investigations are still required. These studies in AF patients used single-beat full volume images to obtain coherent 3D leaflet reconstructions, with a temporal resolution of around 100ms for nine frames/sec. Considering the results of a previous publication (23), the temporal resolution of the current single-beat full volume image should be sufficient. Measurement of LV volumes, function and closure area will vary (beat-to-beat variability) in AF, although values were averaged. The vena contracta dimension and PISA radius are not circular in secondary MR, although we measured this in the standardized planes. The findings apply most specifically to patients with persistent, as opposed to paroxysmal AF. Finally, although we used bootstrap resampling, this can not eliminate inherent problems of a small number of cases and the strength of association may be in part dependent on the unique characteristics of these patients.

Clinical implications

The 4.3% prevalence of significant atrial FMR in this study is comparable to the 6% described by Gertz at al (12). Establishing the presence of atrial FMR and its mechanism is important because it causes clinically important heart failure requiring hospitalization and surgery and may limit the success of ablation and cardioversion procedures (11,19,20). Although MR was reduced in patients undergoing RF ablation without recurrent AF at 1 year relative to those with recurrent AF, there still was 24% significant MR in those with maintained sinus rhythm (12), so that factors other than AF alone may be involved, including more permanent changes to the mitral leaflets in response to altered geometry and stresses. Ultimately, understanding the mechanisms of atrial FMR could lead to both physiologic and potentially mechanical approaches to reduce this complication by encouraging adaptive leaflet growth (1,6), new approaches to leaflet extension(31), percutaneous annular remodeling devices (32) or thermal ablation(33).

These findings are also important to motivate understanding the basic mechanisms of leaflet adaptation and its insufficiency at higher levels of annular dilation. The observed leaflet thickening in the AF groups is consistent with concepts of the inflammatory nature of AF that can alter cellular behavior and growth factor signaling within the leaflets(34). Increased leaflet thickness is consistent with growth through mechanisms such as endothelial-to-mesenchymal transition(6,26), also demonstrated within the LA wall in AF(35). However, leaflet thickening and stiffening, as seen in the post-MI setting (26,36) may also limit adaptive growth and create a vicious cycle of increasing MR and altered valve biology. This will require basic investigations, since leaflet tissue is rarely available in this setting and may not represent early changes. Because an ARB can modulate pro-fibrotic excessive MV EMT *in vitro* (37,38), we noted that in the MR+ patients, those on ACE inhibitors or ARBs had a mildly greater total MLA to closure area ratio and lower VCW than those untreated. However, this is only a suggestive observation that requires mechanistic and experimental studies.

In summary, isolated annular dilation caused by atrial remodeling in AF is associated with active MLA increase, but the compensatory enlargement becomes insufficient at larger AA, causing mild leaflet tenting and increasing MR. Leaflet adaptation also fails to match the disproportionate posterior-predominant annular dilation. These deficiencies of leaflet adaptation are independently associated with the development of significant MR. The findings from this comprehensive 3D analysis can motivate basic studies on adaptive growth processes and may potentially guide optimization of therapeutic options.

Supplementary Material

Refer to Web version on PubMed Central for supplementary material.

Abbreviations

3D	three-dimensional
ARB	angiotensin receptor blocker
ACE	angiotensin converting enzyme
AA	annular area
AF	atrial fibrillation
ESV	end-systolic volume
EDV	end-diastolic volume
FMR	functional mitral regurgitation
MLA	mitral leaflet area
PM	papillary muscle
RF	radio frequency
VCW	vena contracta width

References

1. Beaudoin J, Handschumacher MD, Zeng X, et al. Mitral valve enlargement in chronic aortic regurgitation as a compensatory mechanism to prevent functional mitral regurgitation in the dilated left ventricle. J Am Coll Cardiol. 2013; 61:1809–16. [PubMed: 23500248]
2. Mautner SL, Klues HG, Mautner GC, Proschan MA, Roberts WC, Maron BJ. Comparison of mitral valve dimensions in adults with valvular aortic stenosis, pure aortic regurgitation and hypertrophic cardiomyopathy. Am J Cardiol. 1993; 71:949–53. [PubMed: 8465787]
3. Otsuji Y, Handschumacher MD, Schwammenthal E, et al. Insights from three-dimensional echocardiography into the mechanism of functional mitral regurgitation: direct in vivo demonstration of altered leaflet tethering geometry. Circulation. 1997; 96:1999–2008. [PubMed: 9323092]
4. Yiu SF, Enriquez-Sarano M, Tribouilloy C, Seward JB, Tajik AJ. Determinants of the degree of functional mitral regurgitation in patients with systolic left ventricular dysfunction: A quantitative clinical study. Circulation. 2000; 102:1400–6. [PubMed: 10993859]

5. Chaput M, Handschumacher MD, Tournoux F, et al. Mitral leaflet adaptation to ventricular remodeling: occurrence and adequacy in patients with functional mitral regurgitation. Circulation. 2008; 118:845–52. [PubMed: 18678770]
6. Dal-Bianco JP, Aikawa E, Bischoff J, et al. Active adaptation of the tethered mitral valve: insights into a compensatory mechanism for functional mitral regurgitation. Circulation. 2009; 120:334–42. [PubMed: 19597052]
7. Balachandran K, Alford PW, Wylie-Sears J, et al. Cyclic strain induces dual-mode endothelial-mesenchymal transformation of the cardiac valve. Proc Natl Acad Sci U S A. 2011; 108:19943–8. [PubMed: 22123981]
8. Kim DH, Handschumacher MD, Levine RA, et al. Aortic valve adaptation to aortic root dilatation: insights into the mechanism of functional aortic regurgitation from 3- dimensional cardiac computed tomography. Circ Cardiovasc Imaging. 2014; 7:828–35. [PubMed: 25051951]
9. Sanfilippo AJ, Abascal VM, Sheehan M, et al. Atrial enlargement as a consequence of atrial fibrillation. A prospective echocardiographic study. Circulation. 1990; 82:792–7. [PubMed: 2144217]
10. Otsuji Y, Kumanohoso T, Yoshifuku S, et al. Isolated annular dilation does not usually cause important functional mitral regurgitation: comparison between patients with lone atrial fibrillation and those with idiopathic or ischemic cardiomyopathy. J Am Coll Cardiol. 2002; 39:1651–6. [PubMed: 12020493]
11. Kihara T, Gillinov AM, Takasaki K, et al. Mitral regurgitation associated with mitral annular dilation in patients with lone atrial fibrillation: an echocardiographic study. Echocardiography. 2009; 26:885–9. [PubMed: 19552671]
12. Gertz ZM, Raina A, Saghy L, et al. Evidence of atrial functional mitral regurgitation due to atrial fibrillation: reversal with arrhythmia control. J Am Coll Cardiol. 2011; 58:1474–81. [PubMed: 21939832]
13. Glower DD, Bashore TM, Harrison JK, Wang A, Gehrig T, Rankin JS. Pure annular dilation as a cause of mitral regurgitation: a clinically distinct entity of female heart disease. J Heart Valve Dis. 2009; 18:284–8. [PubMed: 19557984]
14. Kilic A, Schwartzman DS, Subramaniam K, Zenati MA. Severe functional mitral regurgitation arising from isolated annular dilatation. Ann Thorac Surg. 2010; 90:1343–5. [PubMed: 20868842]
15. Hoit BD. Atrial functional mitral regurgitation: the left atrium gets its due respect. J Am Coll Cardiol. 2011; 58:1482–4. [PubMed: 21939833]
16. Ring L, Dutka DP, Wells FC, Fynn SP, Shapiro LM, Rana BS. Mechanisms of atrial mitral regurgitation: insights using 3D transoesophageal echo. Eur Heart J Cardiovasc Imaging. 2014; 15:500–8. [PubMed: 24145456]
17. Machino-Ohtsuka T, Seo Y, Ishizu T, et al. Novel Mechanistic Insights Into Atrial Functional Mitral Regurgitation- 3-Dimensional Echocardiographic Study. Circ J. 2016; 80:2240–8. [PubMed: 27535338]
18. Carpentier A. Cardiac valve surgery--the "French correction". J Thorac Cardiovasc Surg. 1983; 86:323–37. [PubMed: 6887954]
19. Gertz ZM, Raina A, Mountantonakis SE, et al. The impact of mitral regurgitation on patients undergoing catheter ablation of atrial fibrillation. Europace. 2011; 13:1127–32. [PubMed: 21490035]
20. Takahashi Y, Abe Y, Sasaki Y, et al. Mitral valve repair for atrial functional mitral regurgitation in patients with chronic atrial fibrillation. Interact Cardiovasc Thorac Surg. 2015; 21:163–8. [PubMed: 25980774]
21. Kunzelman KS, Cochran RP. Stress/strain characteristics of porcine mitral valve tissue: parallel versus perpendicular collagen orientation. J Card Surg. 1992; 7:71–8. [PubMed: 1554980]
22. May-Newman K, Yin FC. Biaxial mechanical behavior of excised porcine mitral valve leaflets. Am J Physiol. 1995; 269:H1319–27. [PubMed: 7485564]
23. Beaudoin J, Thai WE, Wai B, Handschumacher MD, Levine RA, Truong QA. Assessment of mitral valve adaptation with gated cardiac computed tomography: validation with three-dimensional echocardiography and mechanistic insight to functional mitral regurgitation. Circ Cardiovasc Imaging. 2013; 6:784–9. [PubMed: 23873402]

24. Zoghbi WA, Enriquez-Sarano M, Foster E, et al. Recommendations for evaluation of the severity of native valvular regurgitation with two-dimensional and Doppler echocardiography. J Am Soc Echocardiogr. 2003; 16:777–802. [PubMed: 12835667]
25. Muller H, Reverdin S, Burri H, Shah D, Lerch R. Measurement of left and right atrial volume in patients undergoing ablation for atrial arrhythmias: comparison of a manual versus semiautomatic algorithm of real time 3D echocardiography. Echocardiography. 2014; 31:499–507. [PubMed: 24128369]
26. Dal-Bianco JP, Aikawa E, Bischoff J, et al. Myocardial Infarction Alters Adaptation of the Tethered Mitral Valve. J Am Coll Cardiol. 2016; 67:275–87. [PubMed: 26796392]
27. Kim DH, Handschumacher MD, Levine RA, et al. In vivo measurement of mitral leaflet surface area and subvalvular geometry in patients with asymmetrical septal hypertrophy: insights into the mechanism of outflow tract obstruction. Circulation. 2010; 122:1298–307. [PubMed: 20837895]
28. Blanke P, Dvir D, Cheung A, et al. A simplified D-shaped model of the mitral annulus to facilitate CT-based sizing before transcatheter mitral valve implantation. J Cardiovasc Comput Tomogr. 2014; 8:459–67. [PubMed: 25467833]
29. Song JM, Kim JJ, Ha TY, et al. Basal chordae sites on the mitral valve determine the severity of secondary mitral regurgitation. Heart. 2015; 101:1024–31. [PubMed: 25800999]
30. Jensen MO, Jensen H, Smerup M, et al. Saddle-shaped mitral valve annuloplasty rings experience lower forces compared with flat rings. Circulation. 2008; 118:S250–5. [PubMed: 18824763]
31. Suri RM, Schaff HV. Posterior Leaflet Detachment, Augmentation, and Reconstruction for Treatment of Functional Mitral Valve Regurgitation. Semin Thorac Cardiovasc Surg. 2015; 27:91–4. [PubMed: 26686429]
32. Masson JB, Webb JG. Percutaneous treatment of mitral regurgitation. Circ Cardiovasc Interv. 2009; 2:140–6. [PubMed: 20031707]
33. Rahman S, Eid N, Murarka S, Heuser RR. Remodeling of the mitral valve using radiofrequency energy: review of a new treatment modality for mitral regurgitation. Cardiovasc Revasc Med. 2010; 11:249–59. [PubMed: 20934658]
34. Hu YF, Chen YJ, Lin YJ, Chen SA. Inflammation and the pathogenesis of atrial fibrillation. Nat Rev Cardiol. 2015; 12:230–43. [PubMed: 25622848]
35. Kato T, Sekiguchi A, Sagara K, et al. Endothelial-Mesenchymal Transition in Human Atrial Fibrillation. Circulation. 2014; 130:A13638.
36. Bischoff J, Casanovas G, Wylie-Sears J, et al. CD45 Expression in Mitral Valve Endothelial Cells After Myocardial Infarction. Circ Res. 2016; 119:1215–1225. [PubMed: 27750208]
37. Wylie-Sears J, Levine RA, Bischoff J. Losartan inhibits endothelial-to-mesenchymal transformation in mitral valve endothelial cells by blocking transforming growth factor-beta-induced phosphorylation of ERK. Biochem Biophys Res Commun. 2014; 446:870–5. [PubMed: 24632204]
38. Bartko PE, Dal-Bianco JP, Guerrero JL, et al. Effect of Losartan on Mitral Valve Changes After Myocardial Infarction. J Am Coll Cardiol. 2017; 70:1232–1244. [PubMed: 28859786]

Perspectives

Competency in Medical Knowledge

Mitral leaflet area increase has the potential to adapt to isolated annular dilation in patients with persistent atrial fibrillation and prevent mitral regurgitation; inadequate area increase (insufficient leaflet adaptation), failing to match annular remodeling in extent or asymmetry, can augment tethering and mitral regurgitation

Translational Outlook

These findings can motivate understanding the basic mechanisms of leaflet adaptation. Increased leaflet thickness is consistent with growth through mechanisms such as endothelial-to-mesenchymal transition, also demonstrated within the left atrial wall in atrial fibrillation. We noted that in the patients with mitral regurgitation, those on ACE inhibitors or angiotensin receptor blockers had a mildly greater total mitral leaflet area to closure area ratio and lower vena contracta width than those untreated. However, this is only a suggestive observation that requires mechanistic and experimental studies.

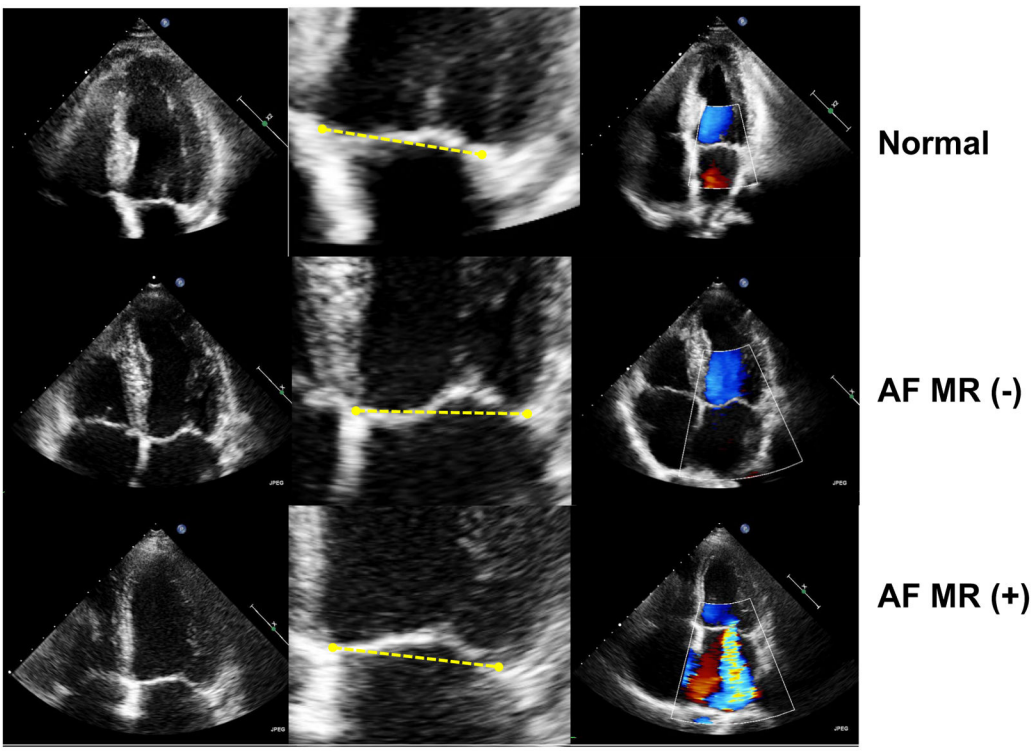

Figure 1. Representative Echocardiographic Images from Each Group

Central column of each row depicts MV tethering relative to the line connecting annular hinge points. The anterior leaflet is concave toward the LV in control and MR-, but relatively flat in MR+ (tethering).

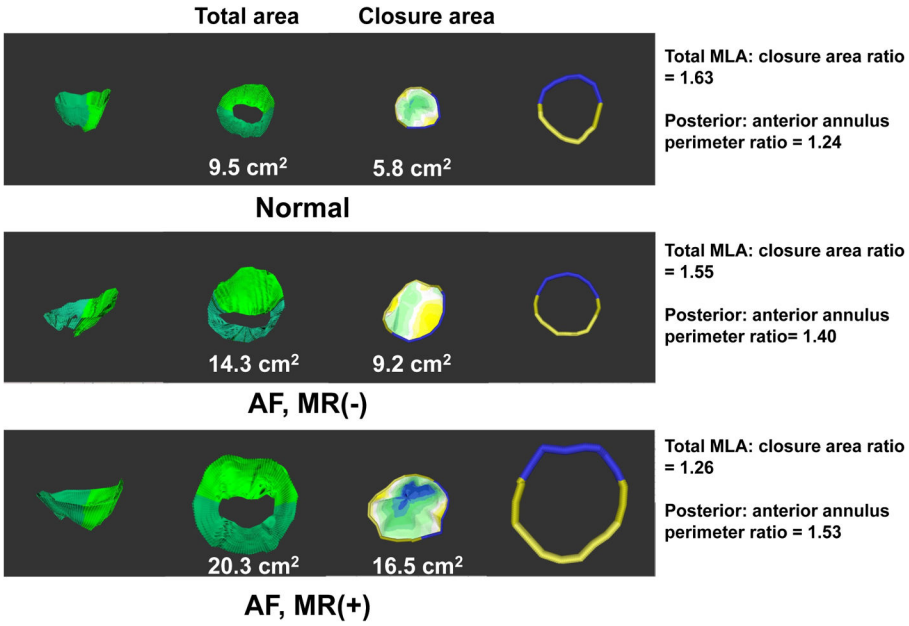

Figure 2. Representative Example of 3-dimensional Reconstructions

1st and 2nd column: side and superior views (larger MLA in AF, greatest in MR+). **3rd column:** closure area with blue (most tented). **4th column:** reconstructed anterior and posterior annuli.

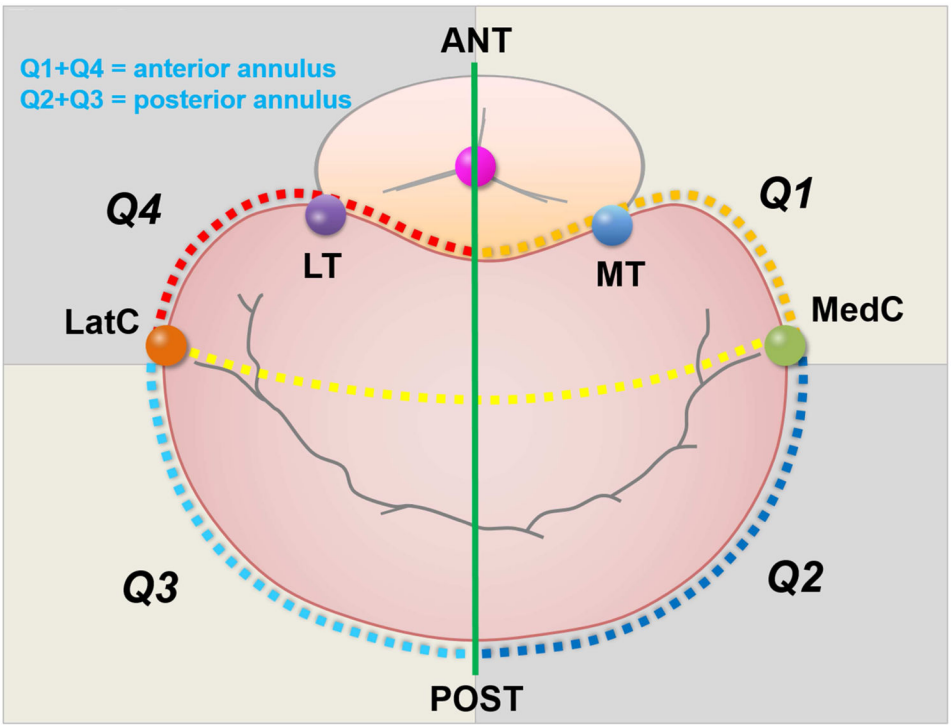

Figure 3. 3D Measurement of Annular Segmental Perimeters in Four Quadrants

Based on medial and lateral commissural points and intersections of annulus with an antero-posterior line connecting AV and MV centroids, posterior and anterior perimeters (Q2+Q3 and Q1+Q4) are measured.

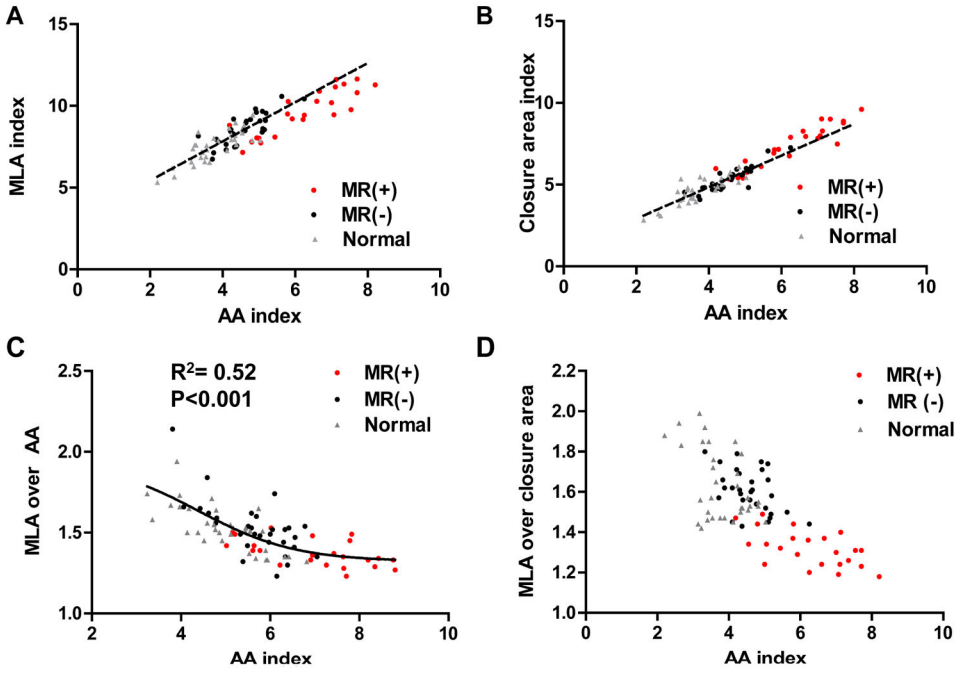

Figure 4. Plateaus in Leaflet Adaptation

(**A**): Total MLA increased in parallel with the AA increase, but declined mildly below the regression line at high AA. (**B**): Closure area likewise increased with AA, but rose mildly above the regression line at high AA. (**C, D**): Total MLA to AA and total MLA to closure area ratios showed lower plateaus at higher AA.

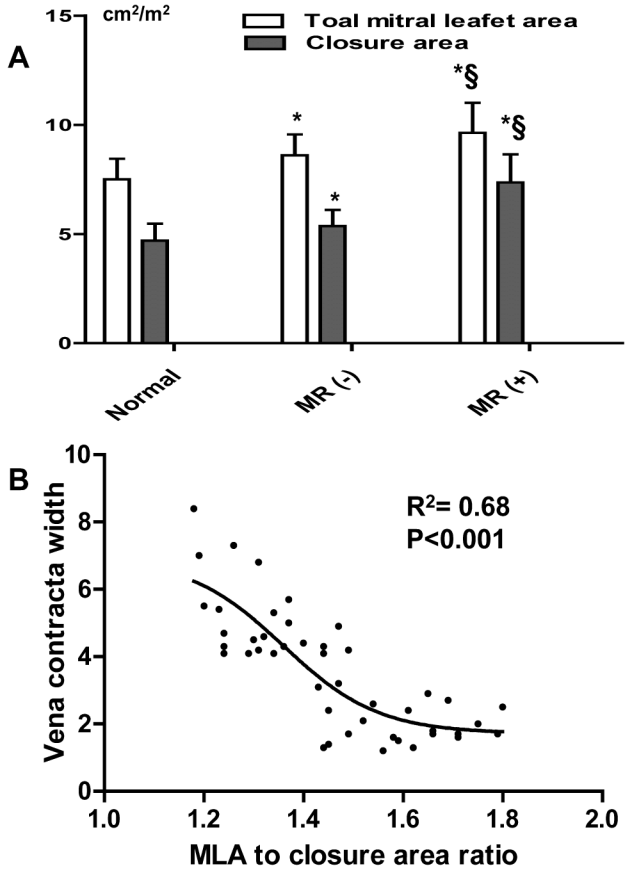

Figure 5. Comparison of Leaflet Areas & Relationship between VCW and Total to Closure Area Ratio

(**A**): Leaflet areas±SD by groups, indicating largest MLAs in MR+ with a disproportionate increased in closure area consistent with tethering. **§:** p-value<0.05 for the difference between MR+ and MR-. *: p-value<0.05 for the difference from normal. **(B):** VCW increases as total to closure leaflet area ratio decreases below the normal range at 1.5.

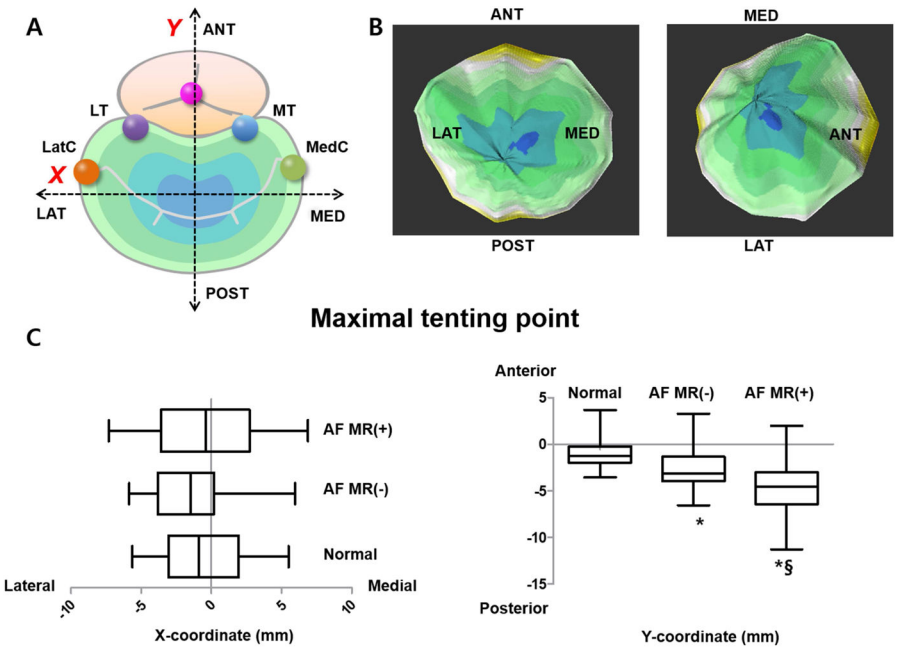

Figure 6. 3D Location of Maximal Tenting Point

(A): Schematic orientation of the maximal tenting point. **(B):** The dark portion indicates the farthest or highest portion from the annulus plane**. (C):** Graphs represent X (medial-lateral distance from the centroid) and Y coordinates (antero-posterior distance) of the maximal tenting point.

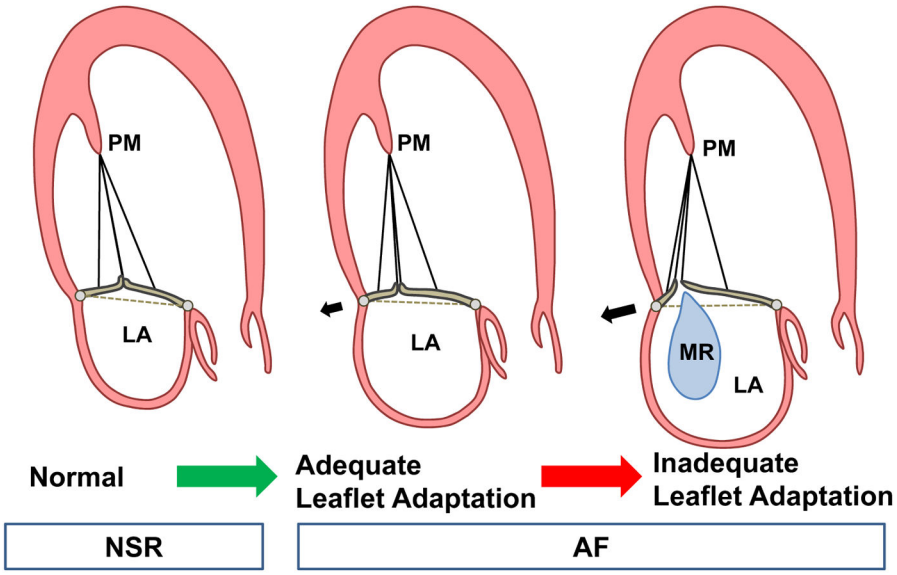

Figure 7. Schematic Illustration of MR Development

MLA increase has the potential to adapt to isolated annular dilation in AF and prevent MR; inadequate adaptation, failing to match annular remodeling in extent, can augment tethering and MR.

Table 1

Baseline characteristics and echocardiographic data of study population

	AF, MR+ (N=23)	AF, MR- (N=30)	Normal Controls (N=33)	*P*
Clinical parameters				
Age, years	68±9	68±8	64±4	0.06
Male gender, %	39	57	46	0.425
BSA, m^2	1.62±0.20	1.67±0.14	1.62±0.16	0.375
SBP, mmHg	*114±8	*115±8	120±7	0.004
DBP, mmHg	*76±5	*77±4	79±4	0.008
Heart rate, BPM	*82±10	79±10	76±7	0.026
Duration of AF, years	6.5±4.5	5.2±3.9	-	0.260 (t-test)
Hypertension, %	22	20	0	0.019
ACEI or ARB use, %	*48	*47	0	<0.001
CCB or BB use, %	*70	*60	0	<0.001
Digoxin use, %	*30	*27	0	<0.001
Echocardiographic parameter				
MR grade, %(n)				
None or trace		87(26)	100(33)	
Mild		13(4)		
Moderate	83(19)			
Severe	17(4)			
LV ESV index, ml/m^2	23.3±7.1	24.2±6.5	20.8±5.1	0.08
LV EDV index, ml/m^2	57.2±12.6	56.0±10.1	56.1±11.7	0.912
LV EF, %	*59.2±6.0	*57.4±7.2	63.3±3.2	<0.001
#3D LA volume index, ml/m^2	§*69.7(28.4)	*49.0(19.1)	30.7(7.9)	<0.001
Anterior leaflet thickness, mm	*2.42±0.41	*2.42±0.36	1.83±0.30	<0.001
Posterior leaflet thickness, mm	*2.54±0.33	*2.43±0.38	1.84±0.43	<0.001

BSA, body surface area; SBP, systolic blood pressure; DBP, diastolic blood pressure; ACEI, angiotensin-converting enzyme inhibitor; ARB, angiotensin receptor blocker; CC, calcium channel blocker; BB, beta-blocker; ESV, end-systolic volume; EDV, end-diastolic volume; EF, ejection fraction.

§ Bonferroni-corrected p-value<0.05 for the difference between MR+ and MR-,

* Bonferroni-corrected p-value<0.05 for the difference from normal controls.

Kruskal-Wallis test was used for the comparison. The numbers being presented are median (interquartile range).

Table 2

Results of omni4D analysis using 3-dimensional echocardiographic data set

	AF, MR+ (N=23)	AF, MR- (N=30)	Normal Controls (N=33)	#P
Mitral leaflet area (MLA)				
Total MLA, cm^2	*§15.5±2.1	*14.3±1.9	12.1±1.5	<0.001
Indexed total MLA, cm^2/m^2	*§9.6±1.4	*8.6±1.0	7.5±0.9	<0.001
Indexed anterior MLA, cm^2/m^2	*§5.4±1.0	*4.8±0.7	4.1±0.6	<0.001
Indexed posterior MLA, cm^2/m^2	*§4.2±0.6	*3.8±0.6	3.4±0.6	<0.001
Anterior to posterior MLA ratio	1.31±0.23	1.30±0.31	1.25±0.20	0.566
Closure area, cm^2	*§11.8±1.8	*9.0±1.4	7.5±1.3	<0.001
Indexed closure area, cm^2/m^2	*§7.4±1.3	*5.4±0.7	4.7±0.8	<0.001
Adaptation-related indices				
Total MLA to annular area ratio	*§1.38±0.10	1.53±0.17	1.53±0.14	<0.001
Total MLA to closure area ratio	*§1.32±0.10	1.60±0.11	1.63±0.17	<0.001
Mitral annulus geometry				
Annular area (diastole) cm^2/m^2	*§6.9±1.4	*5.6±0.8	5.0±0.9	<0.001
Annular area (systole) cm^2/m^2	*§6.3±1.2	*4.6±0.6	3.8±0.7	<0.001
Fractional area change of the MA, %	*§10.6±7.0	*18.4±8.6	23.6±8.7	<0.001
Annular height, mm	*5.3±0.7	*5.0±1.0	6.1±1.0	<0.001
Antero-posterior (AP) diameter, mm/m^2	*§22.0±3.3	*18.4±1.8	16.4±2.0	<0.001
Intercommissural (IC) diameter, mm/m^2	*§21.9±2.8	19.3±1.8	18.4±2.1	<0.001
Non-planarity angle, degrees	*§155.4±6.7	*§149.8±8.2	141.4±8.6	<0.001
Circularity index of annulus	*§1.00±0.11	*0.95±0.06	0.89±0.08	<0.001
Intertrigone distance, mm/m^2	12.9±2.0	12.1±1.7	12.8±1.5	0.243
Total annulus perimeter, mm/m^2	*§78.9±9.6	*73.2±6.0	64.9±7.3	<0.001
Anterior annulus perimeter, mm/m^2	*32.4±5.4	*31.8±3.4	29.1±3.6	0.018
Posterior annulus perimeter, mm/m^2	*§46.5±5.3	*41.4±4.5	35.4±4.3	<0.001

	AF, MR+ (N=23)	AF, MR- (N=30)	Normal Controls (N=33)	#p
Perimeter of Q1, mm/ m^2	16.5±3.2	16.4±2.5	15.0±2.2	0.058
Perimeter of Q2, mm/ m^2	*§23.3±2.8	20.6±3.0	17.8±2.2	<0.001
Perimeter of Q3, mm/ m^2	*§23.2±3.1	*20.1±2.2	17.6±2.8	<0.001
Perimeter of Q4, mm/ m^2	15.9±2.8	15.4±2.1	14.4±2.0	0.05
Posterior to anterior perimeter ratio	*§1.46±0.19	*1.32±0.20	1.21±0.16	<0.001
Q2/Q3 ratio	1.01±0.17	0.99±0.13	1.03±0.16	0.649

Q1, quadrant 1 of mitral annulus; MLA, mitral leaflet area; PM, papillary muscle; MT, medial trigone; MP, medial PM; LP, lateral PM.

§ Bonferroni-corrected p-value<0.05 for difference between MR+ and MR−.

* Bonferroni-corrected p-value<0.05 for difference from normal controls.

p-value of one-way ANOVA or Kruskal-Wallis test across all three groups.

Table 3

Univariate and multivariate logistic regression analysis to identify determinants of significant MR (including three groups)

	Binary logistic regression for MR (Presence or absence of significant MR)					
	Univariate			Multivariate		
	OR	95% CI	P-value	OR	95% CI	P-value
Age	1.04	0.983–1.120	0.149			
Sex	1.606	0.607–4.245	0.340			
BSA	0.347	0.018–6.707	0.483			
ESV index	1.022	0.583–1.022	0.583			
EDV index	1.010	0.967–1.054	0.664			
EF	0.968	0.897–1.045	0.405			
LA volume index	1.098	1.053–1.146	<0.001			
Annular area index	11.127	3.569–34.689	<0.001	5.529	1.517–20.161	0.010
Annular height	0.754	0.465–1.223	0.252			
Fractional area change of the MA	0.840	0.770–0.916	<0.001			
Anterior-posterior (AP) diameter index	2.022	1.464–2.794	<0.001			
Intercommissural (IC) diameter index	1.789	1.333–2.400	<0.001			
Non-planarity angle	1.171	1.076–1.275	<0.001			
Circularity index of annulus *	3.450	1.644–7.238	0.001			
Total annulus perimeter index	1.162	1.075–1.255	<0.001			
Posterior to anterior perimeter ratio *	1.888	1.353–2.643	<0.001	2.371	1.025–5.485	0.044
Q2/Q3 ratio	1.307	0.038–44.990	0.882			
Total MLA index	2.997	1.781–5.043	<0.001			
Closure area index	7.308	2.949–18.112	<0.001			
Total MLA to closure area ratio *	0.139	0.052–0.371	<0.001	0.185	0.053–0.642	0.008
Total MLA to AA ratio *	0.388	0.232–0.648	0.002			
Tenting volume	8.136	2.768–23.913	<0.001			
Anterior tenting angle	1.028	0.935–1.129	0.573			
Posterior tenting angle	1.389	1.192–1.619	<0.001			

	Binary logistic regression for MR (Presence or absence of significant MR)					
	Univariate			Multivariate		
	OR	95% CI	P-value	OR	95% CI	P-value
X-coordinate of maximal tenting point	1.071	0.921–1.245	0.375			
Y-coordinate of maximal tenting point	0.607	0.462–0.797	<0.001			

OR, odds ratio; BSA, body surface area; ESV, end-systolic volume; EDV, end-diastolic volume; EF, ejection fraction; MLA, mitral leaflet area; MT, medial trigone; MP, medial papillary muscle; LT, lateral papillary muscle.

*OR is for 10 unit increases in the independent variable.

Table 4

3D F/U data in a subset of the patients group

Case No.	Time point 1						Time point 2						Time gap, years	Enroll time point
	AA, cm^2	Total MLA, cm^2	Closure area, cm^2	MR grade	MLA/ AA	MLA/ closure area	AA, cm^2	Total MLA, cm^2	Closure area, cm^2	MR grade	MLA/ AA	MLA/ closure area		
1	8.6	12.7	8.3	2	1.48	1.53	10.6	14.3	12.0	3	1.36	1.20	2.8	2
2	11.0	15.9	10.5	2	1.45	1.51	12.9	16.4	13.3	3	1.27	1.24	2.5	2
3	13.8	19.5	12.7	2	1.41	1.53	15.7	20.3	16.5	3	1.29	1.23	2.9	2
4	8.1	13.4	7.7	1	1.64	1.74	10.3	14.1	10.9	3	1.37	1.29	5.3	1
5	7.3	11.1	6.3	1	1.51	1.76	9.5	14.3	9.2	1	1.51	1.55	5.6	1
6	9.6	14.7	8.2	1	1.53	1.79	11.8	18.3	11.5	1	1.55	1.59	4.8	1
7	8.7	15.0	10.2	1	1.73	1.47	11.1	17.2	11.4	1	1.55	1.51	5.5	1